Volumetric Analysis of Vascularized Serous Pigment Epithelial Detachment Progression in Neovascular Age-Related Macular Degeneration Using Optical Coherence Tomography Angiography

Adrian Au,[1] Kirk Hou,[1] Juan Pablo Dávila,[1] Frederic Gunnemann,[2] Serena Fragiotta,[3] Malvika Arya,[4] Riccardo Sacconi,[5] Daniel Pauleikhoff,[2] Giuseppe Querques,[5] Nadia Waheed,[4] K. Bailey Freund,[3] SriniVas Sadda,[6] and David Sarraf[1,7]

[1]Retina Disorders and Ophthalmic Genetics, Stein Eye Institute, University of California-Los Angeles, Los Angeles, California, United States
[2]Department of Ophthalmology, St. Franziskus-Hospital, Münster, Germany
[3]Vitreous Retina Macula Consultants of New York, New York, New York, United States
[4]New England Eye Center, Tufts Medical Center, Boston, Massachusetts, United States
[5]Department of Ophthalmology, IRCCS Ospedale San Raffaele, University Vita-Salute San Raffaele, Milan, Italy
[6]Doheny Image Reading Center, Doheny Eye Institute, Los Angeles, California, United States
[7]Greater Los Angeles VA Healthcare Center, Los Angeles, California, United States

Correspondence: David Sarraf, Stein Eye Institute, 100 Stein Plaza, Los Angeles, CA 90095, USA; sarraf@jsei.ucla.edu.

Submitted: December 19, 2018
Accepted: June 7, 2019

Citation: Au A, Hou K, Dávila JP, et al. Volumetric analysis of vascularized serous pigment epithelial detachment progression in neovascular age-related macular degeneration using optical coherence tomography angiography. *Invest Ophthalmol Vis Sci*. 2019;60:3310–3319. https://doi.org/10.1167/iovs.18-26478

Purpose. To analyze the evolution of type 1 neovascularization associated with vascularized serous pigment epithelial detachment (vsPED) using three-dimensional, volumetric, en face optical coherence tomography angiography (OCTA).

Methods. This was a retrospective case series from four tertiary medical centers. OCTA images were analyzed at baseline and at the 3-, 6-, 12-, 18-, and 24-month follow-up visit when available. Visual acuity, number of injections, PED maximal height and PED area and volume, and choroidal neovascularization (CNV) flow area and progression were determined at each visit. Qualitative and quantitative analysis of CNV progression (including CNV/PED flow area) and final PED morphology was performed to determine anatomic outcomes.

Results. Twenty-four eyes in 22 patients were studied. Median follow-up was 20 months. Across all eyes, maximum PED height decreased from 395.5 to 369.5 µm while CNV/PED flow ratio increased from 27.3% to 40.2%. Median visual acuity was unchanged at 20/40. Final PED outcomes included filled fibrovascular versus persistent vsPED. Filled vsPEDs decreased in PED height and volume and displayed a multilayered morphology in contrast to persistent vsPEDs. Fibrovascular PEDs received on average seven less injections as compared to persistent vsPEDs.

Conclusions. Three-dimensional, volumetric, en face OCTA analysis of vsPED progression illustrated two anatomic outcomes: filled, typically multilayered fibrovascular PED versus persistent vsPED. The filled multilayered PED displayed a reduction in PED height and volume, greater CNV/PED flow ratio, and fewer anti-VEGF injections versus the persistent vsPED and may represent a more stable anatomic outcome while the persistent vsPED may indicate a more unstable morphology.

Keywords: vascularized serous pigment epithelial detachment, age-related macular degeneration, anti-VEGF

Vascularized pigment epithelial detachment (PED) is a common variant of neovascular age-related macular degeneration (AMD) and is most often associated with type 1 neovascularization (NV) previously referred to as occult choroidal neovascularization (CNV).[1–11] Pigment epithelial detachments can assume various morphologic configurations, and a number of different terms have been used to describe PED formation in neovascular AMD, including fibrovascular PED, vascularized serous PED (vsPED), and more recently multilayered PED.[3,12–14] Type 1 NV accounts for up to 40% to 50% of newly diagnosed treatment-naïve patients with exudative AMD.[15] Other studies have noted the presence of the vsPED subtype in 24% to 55% of occult lesions.[15–21]

Traditionally, dye-based fluorescein angiography (FA) has been an integral tool for the diagnosis of PED in neovascular AMD. Gass[14] first described "vascularized serous PEDs" associated with a "flattened" or "notched" border and a "hot spot," a sign of the CNV. In some cases, this hot spot of NV can be more readily identified with indocyanine green angiography (ICGA).[16] Subsequent pivotal clinical trials, most notably the Macular Photocoagulation Study (MPS) and Treatment of Age-Related Macular Degeneration with Photodynamic Therapy

(TAP) described additional morphologic phenotypes of PED associated with "occult" NV, based on FA, including "fibrovascular" subtypes characterized by "stippled leakage" or "late ooze."[3,12,22,23] While these studies assumed progressive growth of type 1 NV through the PED, the sequential evolution of this process has never been precisely illustrated or validated.

Both FA and ICGA lack depth resolution in three dimensions and poorly display neovascular membranes within PEDs, hence the designation "occult."[14] Optical coherence tomography (OCT) and OCT angiography (OCTA) provide depth-resolved capability and enhanced microvascular resolution of type 1 NV through the PED and present an opportunity for the first time to sequentially study the evolution of NV in association with a PED and gain insight into the mechanisms of progression.[6,13,24–26] Three-dimensional volumetric OCT and OCTA reconstruction may be especially powerful to display the dynamic interplay and progression of NV within the PED.[27] Given the noninvasive nature and ease and facility of scan acquisition, frequent follow-up imaging can be performed to precisely monitor the evolution and progression of type 1 NV associated with PED and its morphologic response to anti-VEGF therapy. Thus, this study aimed to describe the morphologic growth patterns of type 1 NV associated with serous PED and to evaluate how NV affects PED structural dynamics in the setting of anti-VEGF therapy using en face OCT and OCTA.

Methods

This retrospective case series was approved by the Institutional Review Board at the University of California-Los Angeles, adhered to the Health Insurance Portability and Accountability Act, and was performed in accordance with the Declaration of Helsinki. Informed consent was obtained from all patients who underwent OCTA.

Patients were evaluated between January 1, 2015 and January 1, 2018 at one of four retinal centers (Stein Eye Institute, Los Angeles, CA, USA; St. Franziskus-Hospital, Münster, Germany; Vitreous Retina Macula Consultants of New York, NY, USA; New England Eye Center, Tufts Medical Center, Boston, MA, USA). Inclusion criteria included a diagnosis of neovascular AMD, presence of a vsPED at baseline, follow-up of at least 6 months, and OCTA scans at baseline and follow-up with quality index of 5 or higher and signal strength index of at least 45 or greater (RTVue XR Avanti AngioVue OCTA Version 2017.1.0.151; Optovue, Inc., Fremont, CA, USA). Either or both eyes were eligible for inclusion. Patients were included if they had a minimum of 6 months of follow-up. OCTA scans were analyzed at baseline and at the 3-, 6-, 12-, 18-, and 24-month follow-up, when available. However, given the variability in follow-up, patients were analyzed at baseline and final visit. Patients were excluded if any evidence of type 2 or 3 NV was present with OCT or OCTA at any study visit. Eyes with other confounding retinal disease such as diabetic retinopathy or retinal vein occlusion were also excluded.

Each patient underwent ophthalmic examination and multimodal retinal imaging. All patients were imaged with spectral-domain OCT and OCTA at all study visit intervals. Dye-based FA and ICGA and fundus autofluorescence were performed in only selected patients but were not required for this analysis. The dosing regimen, pro re nata versus treat and extend, and frequency of intravitreal anti-VEGF injections were determined by the treating physician according to the presence of hemorrhage and/or intra- or subretinal fluid. Split-spectrum decorrelation algorithm OCTA (Optovue RTVue XR Avanti; Optovue, Inc.) with three-dimensional projection artifact removal was performed on each eye. OCTA scans (3 $\times$ 3 or 6 $\times$ 6 mm) were analyzed using a manual segmentation of the retinal pigment epithelium (RPE) contour of the PED at each OCTA visit. Additional clinical data collected for each patient included age, sex, best-corrected visual acuity (Snellen and converted into logMAR), and history of intravitreal anti-VEGF injections.

OCTA segmentation along the hyperreflective RPE and Bruch's membrane bands was manually evaluated and corrected if misaligned. Two segmentation parameters were used to analyze the PEDs. Alignment along RPE to Bruch's membrane was used for volumetric analysis of the PED. Alignment along RPE to RPE with a 30-μm offset beneath the RPE was employed for flow analysis of the associated type 1 NV in the PED. Three-dimensional reconstruction with this segmentation was performed utilizing the automated RTVue XR Avanti AngioVue OCTA Version 2017.1.0.151 (Optovue, Inc.) software maintaining the same segmentation as above. Initial segmentation offset was determined on presentation by localizing the maximal serous component on en face OCT. This segmentation was then maintained throughout each follow-up visit. Maximum PED height was manually measured from the RPE to Bruch's membrane independently by two graders (A.A., K.H.) and discrepancies greater than 10 μm were evaluated by a third grader (J.P.D.). Optovue ReVue software algorithm calculated PED volume by assessing the difference between Bruch's and RPE across the entire PED. Choroidal neovascularization/pigment epithelial detachment (CNV/PED) flow ratio was calculated as the ratio of NV flow area to total PED area. NV flow area was determined by exporting and analyzing aligned en face OCT and OCTA scans in ImageJ (National Institutes of Health, Bethesda, MD, USA). Total PED area was manually ascertained by demarcating the borders of the PED with en face OCT with the built-in Optovue ReVue flow tool. All images were exported through the built-in multiscan function so that segmentation remained tracked between visits. The area of the PED as outlined with en face OCT was then overlaid on the corresponding en face OCTA. This area was selected and added to the region of interest (ROI) manager prior to thresholding to ensure consistency of selection. Images were converted to 8 bits and thresholded based on the average of the three lowest signals within the NV area of the baseline OCTA. As each multiscan image already contained all follow-up tracked OCTA images with the same segmentation, flow area was then calculated (Fig. 1).

Diagnosis of vsPED was established with en face and cross-sectional spectral-domain OCT in which the hyporeflective serous component comprised greater than 60% $\pm$ 5% of the PED by CNV/PED flow ratio at baseline. Progressive growth of the choroidal neovascular membrane in the PED was mapped and measured at each follow-up visit. Adjacent type 1 NV was determined by presence of NV that was continuous with the vsPED identified with en face OCTA and OCT B-scan analysis. Presence of a neovascular monolayer was defined as identification of uniform hyperreflectivity of less than 10 μm beneath the RPE with corresponding angiographic flow on OCTA. This determination was made by evaluating the sequential cross-sectional and en face OCT and OCTA images to evaluate the depth of the NV in three dimensions. Progression to filled fibrovascular PED was defined as CNV/PED flow ratio greater than 60% at any follow-up visit; otherwise a designation of persistent vsPED was made. Reduction in PED height was defined as a greater than 100-μm decrease in PED height. OCT characteristics that describe multilayered fibrovascular PED, specifically the identification of a fibrovascular and fibrocellular component and a choroidal cleft, were established as previously described.[13,28] Briefly, the fibrovascular component was defined as an irregular, heterogeneous hyperreflective layer immediately beneath the RPE, and the fibrocellular

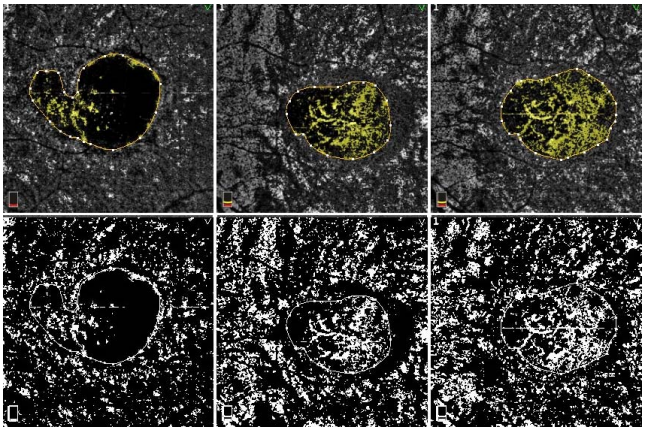

FIGURE 1. Methodology of analysis of CNV/PED flow ratio. Baseline and follow-up en face OCTA (*top*) images that are tracked and identically segmented. Note the delineation of the PED border and the area of associated neovascularization using the Optovue built-in software. Borders were determined by overlay of the en face structural OCT. Prior to conversion, ROIs were preselected and stored in the ROI manager in ImageJ. The image was then converted to an 8-bit grayscale image and thresholded based on the average of the three lowest flow signals on the baseline images. The resultant images (*bottom*) were then measured for the signal within the PED, which is determined as the neovascular area. CNV/PED flow ratio is subsequently calculated as the neovascular area divided by the PED total area.

component was defined as smooth fusiform or spindle-shaped hyperreflectivity immediately below the fibrovascular layer on cross-sectional OCT. A prechoroidal cleft was noted if uniform hyporeflectivity was identified beneath the fibrocellular component (Fig. 2). RPE tear was defined as an interrupted RPE band noted with cross-sectional OCT.[29] Atrophy was defined based on the recent consensus definition of complete RPE and outer retinal atrophy by OCT comprising a region of hypertransmission of 250 μm in diameter associated with complete RPE and outer retinal loss in the absence of scrolled RPE or other signs of an RPE tear.[30]

Results are reported as medians with range or number with percentage. Categorical variables were analyzed with χ^2 test, while independent *t*-tests were performed for interval variables. Given the variability in follow-up between patients, CNV flow area, CNV/PED flow ratio, and PED height and volume versus follow-up were graphed with trend lines to indicate the positive or negative slope. Statistical analysis was performed within Excel (Microsoft, Redmond, WA, USA). A *P* value of <0.05 was considered statistically significant.

RESULTS

Patient Characteristics

Twenty-four eyes from 22 patients were evaluated and demographic data are summarized in Table 1. Across all patients, average age was 77.2 years (57.0–97.5 years); 70.8% of subjects were female (17/24) and median follow-up was 20 months (6.5–26.3 months). Analysis was performed on 110 OCTs and 110 OCTAs to determine the PED phenotype. Twelve eyes were characterized as a persistent vsPED throughout the follow-up and 12 eyes evolved into a filled fibrovascular PED. Both groups were predominantly female with an equal distribution of right and left eyes ($P = 0.66$ and 0.42, respectively). Median follow-up period was 17.2 months (8.9–24.3 months) in the fibrovascular group and 22.3 months (6.5–26.3 months) in the persistent vsPED group ($P = 0.45$).

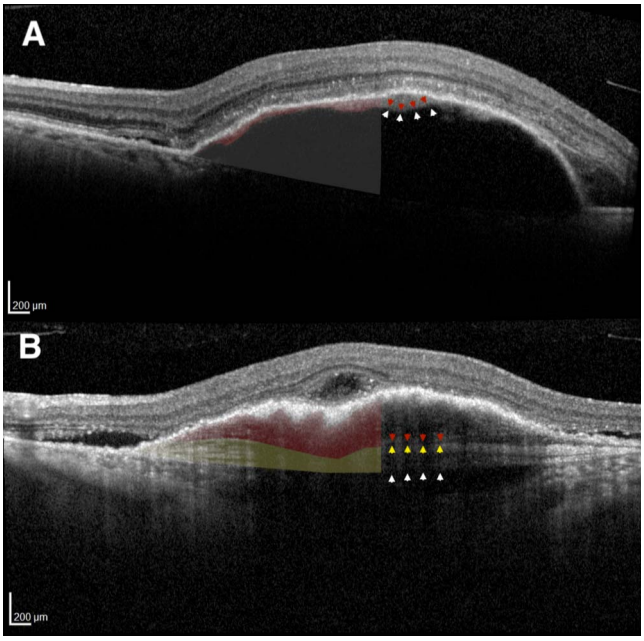

FIGURE 2. Phenotypic comparison of vascularized serous versus fibrovascular PED. A cross-sectional B-scan OCT of a vsPED (**A**) illustrates the fibrovascular membrane growing directly beneath the RPE (*red*) that is distinct from the serous component (*white*). By contrast, the B-scan OCT of the fibrovascular PED (**B**) shows a distinct multilayered PED phenotype. The fibrovascular component (*red*) is beneath the RPE, which contains an irregular, heterogenous hyperreflective layer that includes the neovascular membrane. Just beneath is the fibrocellular portion (*yellow*) of the NV complex, which displays a distinct fusiform or spindle-shaped hyperreflectivity. Lastly, the prechoroidal cleft is a nonreflective potential space (*white*). The *arrowheads* delineate the border of each layer.

Eyes with persistent vsPED were less commonly treatment naïve (58.3%) versus those that developed into fibrovascular PED (25.0%, $P = 0.02$). A median of 6.5 fewer injections were performed in the fibrovascular PED group versus the persistent vsPED group ($P = 0.01$) prior to the study period. Patients with vsPED that progressed to fibrovascular PED received a median of three fewer injections over 20 months as compared to patients with persistent vsPED, but this difference did not meet statistical significance ($P = 0.16$).

Evolution of Neovascularization in the Pigment Epithelial Detachment

Baseline type 1 NV was predominantly located near the margin of the vsPED in 70.8% of all study eyes (Table 1). When not located at the edge of the vsPED, NV was identified central within the PED. Over the 20-month follow-up, CNV flow signal area statistically increased across all eyes from a median of 1.0 (0.04–7.7 mm^2) to 2.7 mm^2 (0–11.2 mm^2, $P = 0.007$, Table 2). Comparison CNV flow area change between persistent vsPED and fibrovascular PED showed no statistical significance ($P = 0.09$, Table 3; Fig. 3). The serous PED in all eyes had a baseline median CNV/PED flow ratio of 27.3% (6.1%–44.9%) and final CNV/PED flow ratio of 40.2% (11.8%–90.3%, $P = 0.006$, Table 2). Subanalysis of CNV/PED flow ratio change indicated CNV/PED flow ratio progression in both vsPEDs that developed into fibrovascular PEDs (24.5%, −15.2% to 76.2%) and in persistent vsPEDs (3.1%, −15.5% to 23.7%), although CNV/PED flow ratio progression was significantly greater in the former ($P = 0.01$, Table 3; Fig. 4). In one case, a −15.2% change in CNV/PED flow

Table 1. Patient Demographic Characteristics and Baseline PED Structure

Characteristics	Total, 24	Fibrovascular PED, 12	Persistent vsPED, 12	*P* Values
Age, y, median (range)	77.2 (57.0–97.5)	77.6 (61.3–91.6)	72.2 (57.0–97.5)	0.80*
Sex				
Male, No. (%)	7 (29.2)	4.0 (33.3)	3.0 (25)	0.66†
Female, No. (%)	17 (70.8)	8.0 (66.7)	9.0 (75)	0.66†
Eye				
Right, No. (%)	12 (50)	5.0 (41.7)	7.0 (58.3)	0.42†
Left, No. (%)	12 (50)	7.0 (58.3)	5.0 (41.7)	0.42†
Follow-up, mo, median (range)	20 (6.5–26.3)	17.2 (8.9–24.3)	22.3 (6.5–26.3)	0.45*
Total injections, No., median (range)	8 (0–46)	8 (0–21)	11 (0–46)	0.16*
Treatment naïve, No. (%)	10 (41.6)	3 (25.0)	7 (58.3)	0.02†
Prior injections, No., median (range)	0 (0–27)	0 (0–3)	6.5 (0–27)	0.01*
Adjacent type 1 NV, No. (%)	17 (70.8)	9 (75.0)	8 (66.7)	0.66†
NV monolayer, No. (%)	22 (91.5)	11 (91.5)	11 (91.5)	1.00†
Baseline				
CNV flow area, mm^2, median (range)	1.0 (0.04–7.7)	0.9 (0.2–3.5)	1.2 (0.04–7.7)	0.27*
CNV/PED flow ratio, %, median (range)	27.3 (6.1–44.9)	27.0 (11.8–44.8)	27.4 (6.1–44.9)	0.83*
PED height, μm, median (range)	395.5 (105.0–684.0)	425.5 (110.0–684.0)	339.0 (105.0–547.0)	0.49*
PED volume, mm^2, median (range)	1.4 (0.2–3.7)	1.72 (0.2–3.7)	1.1 (0.4–2.8)	0.49*
LogMAR, median (range)	0.3 (0.0–0.8)	0.3 (0.0–0.6)	0.3 (0.1–0.8)	0.97*

* Student's *t*-test.
† χ^2 test.

ratio was noted in the fibrovascular PED group due to the development of an RPE tear and subsequent atrophy.

When evaluating the NV in three dimensions, the neovascular lesion presented initially as a monolayer beneath the RPE (91.5%, Table 1). Of the 12 fibrovascular PED eyes, 10 eyes (83%) showed multilayering of the neovascular membrane. An example of a multilayered PED is illustrated in Figure 2. In the other two cases, the serous PED reduced in height due to an RPE tear or collapsed with no evidence of multilayered NV.

Vascularized Serous PED Outcomes

In all 24 eyes, the average PED maximum height was 395.5 μm (105.0–684.0 μm) and volume was 1.4 mm^2 (0.2–3.7 mm^2, Table 1). There was no statistically significant difference between the fibrovascular and persistent vsPED groups as it pertains to baseline PED height, volume, or CNV flow area, or CNV/PED flow ratio ($P = 0.49$, 0.49, 0.27, 0.83 respectively, Table 1). There was an overall decrease in PED height to 369.5 μm (0.0–651.0 μm) and PED volume to 0.9 mm^2 (0.02–4.5 mm^2, Table 2). There was a statistically significant decrease in the height of the PED that became fibrovascular (–156.0 μm, –33.0 μm to –156.0 μm, Table 3; Fig. 5) as compared to a mild increase in height in the persistent vsPED group (27.5 μm, –60.0 to 326.0 μm, $P < 0.001$, Table 3; Fig. 5). These findings were validated with PED volumetric analysis. A reduction in PED volume of –0.52 mm^2 (–2.7 to 1.4 mm^2) was noted in the fibrovascular PED group versus an increase of 0.07 mm^2 (–0.31 to 3.1 mm^2) in the persistent vsPED group ($P = 0.02$, Table 3, Fig. 6). Nearly all vsPEDs that evolved to a fibrovascular PED displayed significant reduction in height (83.3%, Table 3) while only one persistent vsPED displayed significant reduction ($P = 0.0003$). One fibrovascular PED developed a grade 3 RPE tear and subsequent atrophy during the study period. One eye in the persistent vsPED group developed a grade 3 RPE tear.

Visual Acuity Remained Stable Across All Vascularized Serous PEDs

The median baseline visual acuity across all eyes in logMAR was 0.3 (Snellen 20/40, range, 0.0–0.8, Table 1) with no significant difference between fibrovascular and persistent vsPED groups ($P = 0.97$, Table 1). Final best-corrected visual acuity across all eyes remained stable at 0.3 (Snellen 20/40, range, 0.0–1.3, $P = 0.34$, Table 2). Subanalysis between groups indicated that the visual acuity remained stable in both fibrovascular and persistent vsPED with no difference between groups ($P = 0.58$, Table 3).

Cases

Case 1: Persistent Vascularized Serous PED (Fig. 7). A 70-year-old male with neovascular AMD in the right eye presented with a prior history of 17 intravitreal aflibercept injections. At baseline examination, visual acuity was 0.1 (Snellen 20/25) and baseline OCT and OCTA with three-dimensional reconstruction illustrated a vsPED with approximately 10% CNV/PED flow ratio in the temporal macular

Table 2. Pigment Epithelial Detachment (PED) Structural Measurements and Visual Acuity at Baseline and Final Follow-Up As Assessed in Entire Cohort

	Baseline, 24	Final, 24	*P* Values*
CNV flow area, mm^2, median (range)	1.0 (0.04–7.7)	2.7 (0–11.2)	0.007
CNV/PED flow ratio, %, median (range)	27.3 (6.1–44.9)	40.2 (11.8–90.3)	0.006
PED height, μm, median (range)	395.5 (105.0–684.0)	369.5 (0.0–651.0)	0.09
PED volume, mm^2, median (range)	1.4 (0.2–3.7)	0.9 (0.02–4.5)	0.50
LogMAR, median (range)	0.3 (0.0–0.8)	0.3 (0.0–1.3)	0.34

* Student's *t*-test.

Table 3. Comparison of Pigment Epithelial Detachment Anatomic Outcomes and Visual Acuity for Persistent vsPED Group Versus Fibrovascular PED Group

	Fibrovascular PED, 12	Persistent vsPED, 12	*P* Values*
Height reduction, No. (%)	10 (83.3)	1 (8.3)	0.0003
Atrophy, No. (%)	1 (8.3)	0 (0.0)	0.32
RPE tear, No. (%)	1 (8.3)	1 (8.3)	1.0
Δ CNV flow area, mm^2, median (range)	1.0 (−1.3 to 4.9)	0.4 (−0.7 to 1.3)	0.09
Δ CNV/PED flow ratio, %, median (range)	24.5 (−15.2 to 76.2)	3.1 (−15.5 to 23.7)	0.01
Δ PED height, μm, median (range)	−156 (−33.0 to −156.0)	27.5 (−60.0 to 326.0)	<0.001
Δ PED volume, mm^2, median, (range)	−0.52 (−2.7 to 1.4)	0.07 (−0.31 to 3.1)	0.02
Δ LogMAR, median (range)	0.0 (−1.1 to 0.4)	0.0 (−0.4 to 0.4)	0.58

* χ^2 test.

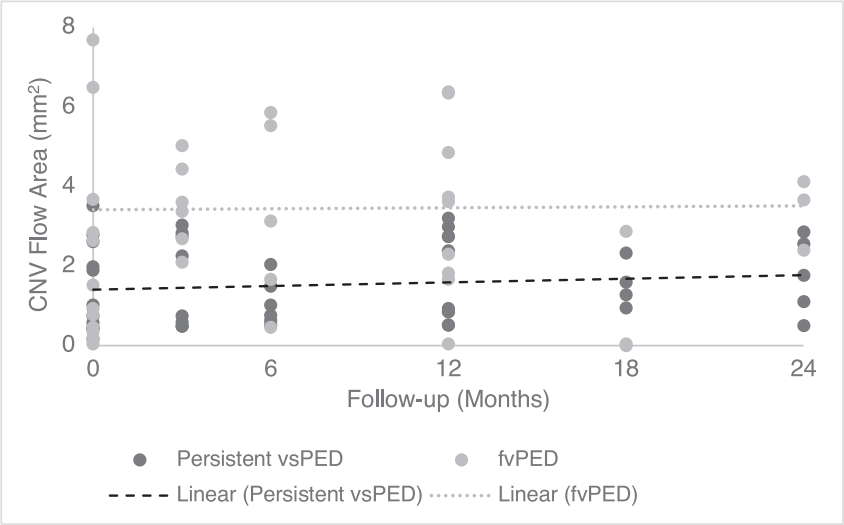

Figure 3. CNV flow area versus follow-up in the persistent vsPED and fibrovascular PED subgroups. Trend lines are included to compensate for the variable follow-up. Note the small but positive slope in CNV flow area in both fibrovascular and persistent vascularized serous groups.

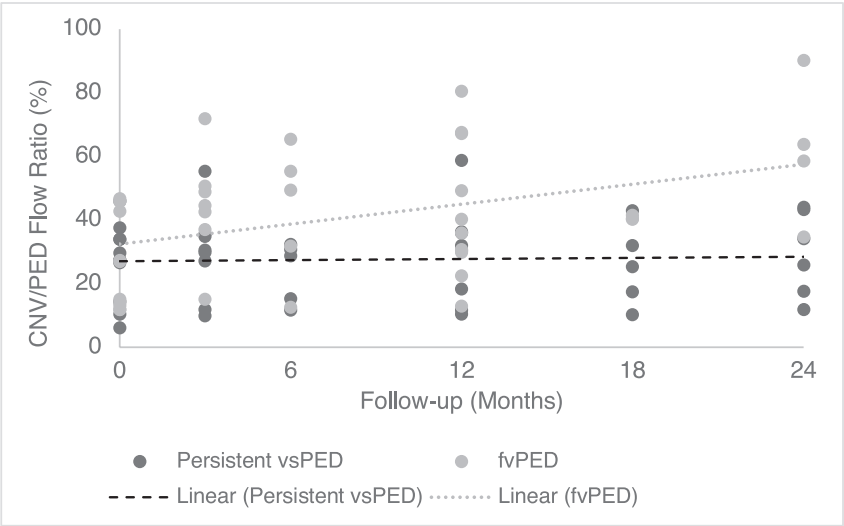

Figure 4. CNV/PED flow ratio versus follow-up in the persistent vsPED and fibrovascular PED subgroups. Trend lines are included to compensate for the variable follow-up. Note the positive slope indicating progression in the CNV/PED flow area only in the fibrovascular PED group.

Investigative Ophthalmology & Visual Science

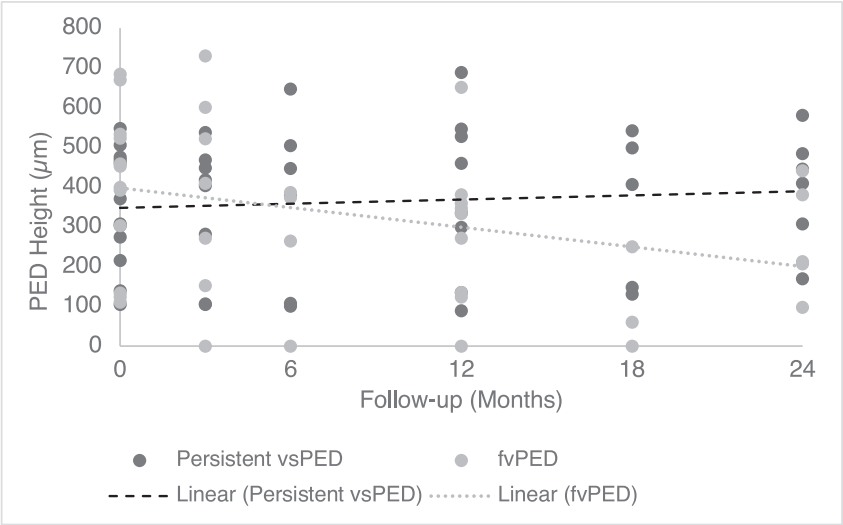

Figure 5. PED height versus follow-up in the persistent vsPED and fibrovascular PED subgroups. Trend lines are included to compensate for the variable follow-up. Note the decreasing slope indicating decreasing PED height in the fibrovascular PED group.

region. Adjacent type 1 CNV was located in the central macula at the edge of the vsPED located temporal to the fovea right eye (Figs. 7A, 7D, 7G). At the 1- and 2-year follow-up visits, the overall area and volume of the temporal vsPED increased with a corresponding increase in the CNV/PED flow ratio (from 10% to approximately 35%) but the maximal PED height was stable (Figs. 7B, 7E, 7H and Figs. 7C, 7F, 7I, respectively). During the evaluation period, the patient received 13 aflibercept injections and final visual acuity was stable at 0.3.

Case 2: Progression of Vascularized Serous PED to Fibrovascular PED With a Multilayered PED Morphology and PED Height Reduction (Fig. 8). An 81-year-old male with neovascular AMD and three prior intravitreal aflibercept injections in the right eye presented with a baseline visual acuity of 0.4 (Snellen 20/50). A vsPED with a CNV/PED flow ratio of 14.0% was identified with initial OCT and OCTA with three-dimensional reconstruction (Figs. 8A, 8D, 8G). A significant increase in CNV/PED flow ratio (80.5%) and decrease in total volume (33%) and PED height (27%) at 1-year follow-up was noted after 10 additional intravitreal aflibercept injections. A multilayered PED configuration was identified (Fig. 8E). At the 2-year follow-up, the overall PED volume decreased to 93% of presentation with a further increase in the CNV/PED flow ratio to 90.3% (Figs. 8C, 8F, 8I). Final visual acuity was 0.1 (Snellen 20/25).

Case 3: Progression of Vascularized Serous PED to Fibrovascular PED Without PED Height Reduction (Fig. 9). A 79-year-old female with treatment-naïve neovascular AMD in the left eye presented with a vsPED with multimodal imaging (Figs. 9A, 9D, 9G). Visual acuity at presentation was 0.4 and flow area was 21.1%. After six monthly injections of intravitreal aflibercept, the vsPED progressed to a multilayered fibrovascular PED with a significant increase in the CNV/PED flow ratio (55.4%) and a minimal increase in PED volume (9%) and PED height (6.7%) (Figs. 9B, 9E, 9H). After 2 years and an additional six intravitreal aflibercept injections, the CNV/PED flow ratio increased (70.3%) while the PED height and volume remained stable compared to the 6-month follow-up. The multilayered morphology was even more prominent. Final visual acuity was 0.7 (Snellen 20/100) (Figs. 9C, 9F, 9I).

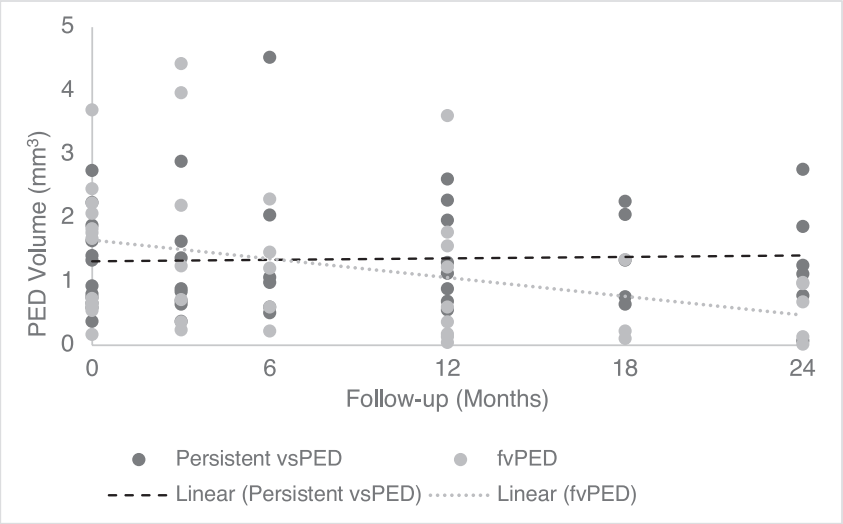

Figure 6. PED volume versus follow-up in the persistent vsPED and fibrovascular PED subgroups. Trend lines are included to compensate for the variable follow-up. Note the decreasing slope indicating decreasing PED volume in the fibrovascular PED group.

Investigative Ophthalmology & Visual Science

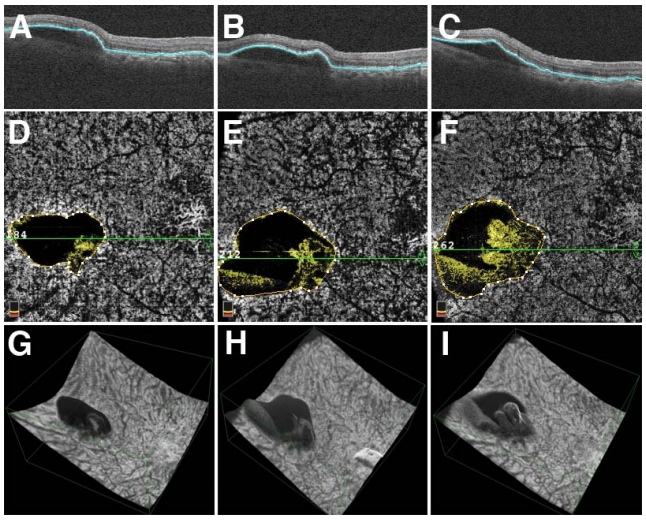

FIGURE 7. Persistent vsPED without reduction in height. Cross-sectional OCT, en face OCTA, and three-dimensional reconstruction at baseline (**A**, **D**, **G**), 1-year (**B**, **E**, **H**), and 2-year (**C**, **F**, **I**) follow-up. The OCT B-scan illustrates a vsPED that remains stable in maximum PED height (**A–C**); however, CNV/PED flow ratio increases with OCTA (**D–F**) and with three-dimensional reconstruction (**G–I**).

Cases 4 and 5: Two Different Cases of PED Height Reduction Are Illustrated (Fig. 10). Case examples of acute versus chronic PED collapse are presented with sequential cross-sectional OCT B-scans in Figure 10. Both patients displayed vsPED at baseline (Figs. 10A, 10B). In the case of acute PED collapse, the serous component of the vsPED, which was treatment naïve, resolved after the first injection (Fig. 10B). At the 2- and 4-month follow-up visits, the serous component recurred despite two additional anti-VEGF injections (Figs. 10C, 10D, respectively). At the 6-month follow-up, the PED collapsed again, exhibiting signs of a fibrovascular PED (Fig. 10E). In the second case, by contrast, the vsPED did not collapse after anti-VEGF therapy and evolved into a multilayered fibrovascular PED. After the first three injections, the vsPED at the 3-month follow-up visit displayed a multilayered morphology with PED height reduction (Fig. 10F). This multilayered appearance remained stable at 4 months (Fig. 10G), 1 year (Fig. 10H), and 2 years (Fig. 10I) with seven interval injections.

DISCUSSION

In this study, we analyzed the evolution of a vsPED, using volumetric, three-dimensional OCT angiography in a serial longitudinal analysis. We determined quantitative values for the natural progression of type 1 NV within a vsPED and we demonstrated the morphologic outcomes of a vsPED treated with intravitreal anti-VEGF therapy, which included persistent vsPED versus filled multilayered fibrovascular PED. In the majority of eyes with vsPED at baseline, the CNV developed at the margin of the PED and progressively grew into the PED along the RPE monolayer. While the CNV/PED flow ratio increased and the serous component decreased in almost all eyes, this was most marked in the vsPEDs that evolved to the multilayered fibrovascular form. These outcomes may have implications regarding pathophysiological mechanisms and management of PEDs.

This study provided evidence for two distinct morphologic phenotypes that evolve from vsPEDs in eyes with neovascular AMD treated with anti-VEGF therapy. Vascularized serous PEDs either progressed to a multilayered fibrovascular form predominantly filled by the type 1 NV complex or persisted as a vsPED in which the majority of the PED remained serous. The fibrovascular multilayered PED, unlike the persistent vsPED, more commonly collapse as illustrated by significant reduction in PED height and volume. The neovascular complex within the persistent vsPED displayed limited growth, and this growth rate was significantly lower than the NV growth rate in the fibrovascular PED group. The fact that the persistent vsPED eyes were less likely to be treatment naïve, had more injections prior to the study period, and required more injections during

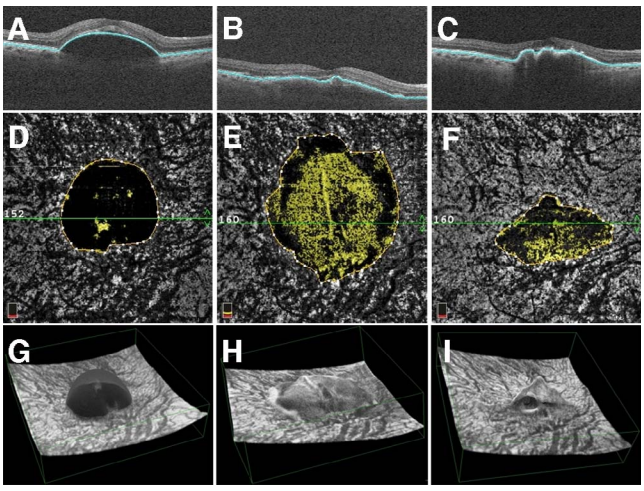

FIGURE 8. Progression of vsPED to multilayered fibrovascular PED that reduced in height. Cross-sectional OCT illustrates the presence of a vsPED at baseline (**A**) that reduces in height at 1 year (**B**) with RPE wrinkling at the 2-year follow-up (**C**) indicating an increasing proportional area of type 1 neovascularization as illustrated with OCTA (**D–F**). Three-dimensional reconstruction displays the subtle hyperreflectivity at baseline, indicating the initial focus of neovascularization that subsequently progresses through the PED in a multilayered morphology (**G–I**).

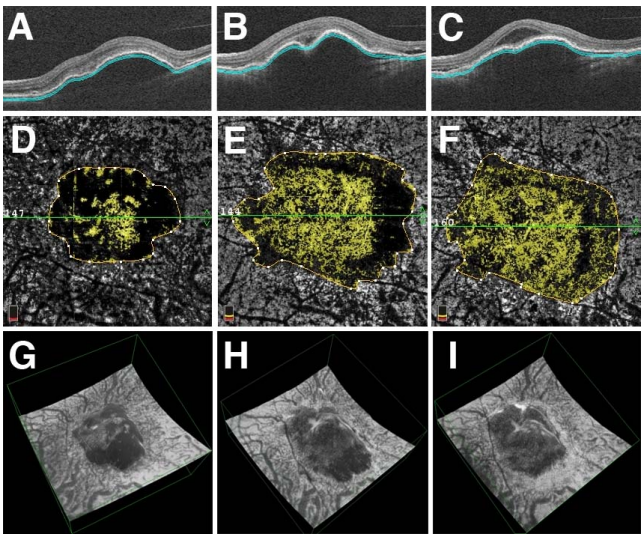

FIGURE 9. Progression of vsPED to fibrovascular PED without height reduction. The cross-sectional OCT illustrates a vsPED at baseline (**A**) that progresses to a multilayered fibrovascular PED at 1-year (**B**) and 2-year (**C**) follow-up visits. The multilayered morphology is illustrated at the 2-year follow-up (**C**). These changes develop concurrently with increasing flow of the NV through the PED with OCTA (**D–F**) and with three-dimensional reconstruction (**G–I**).

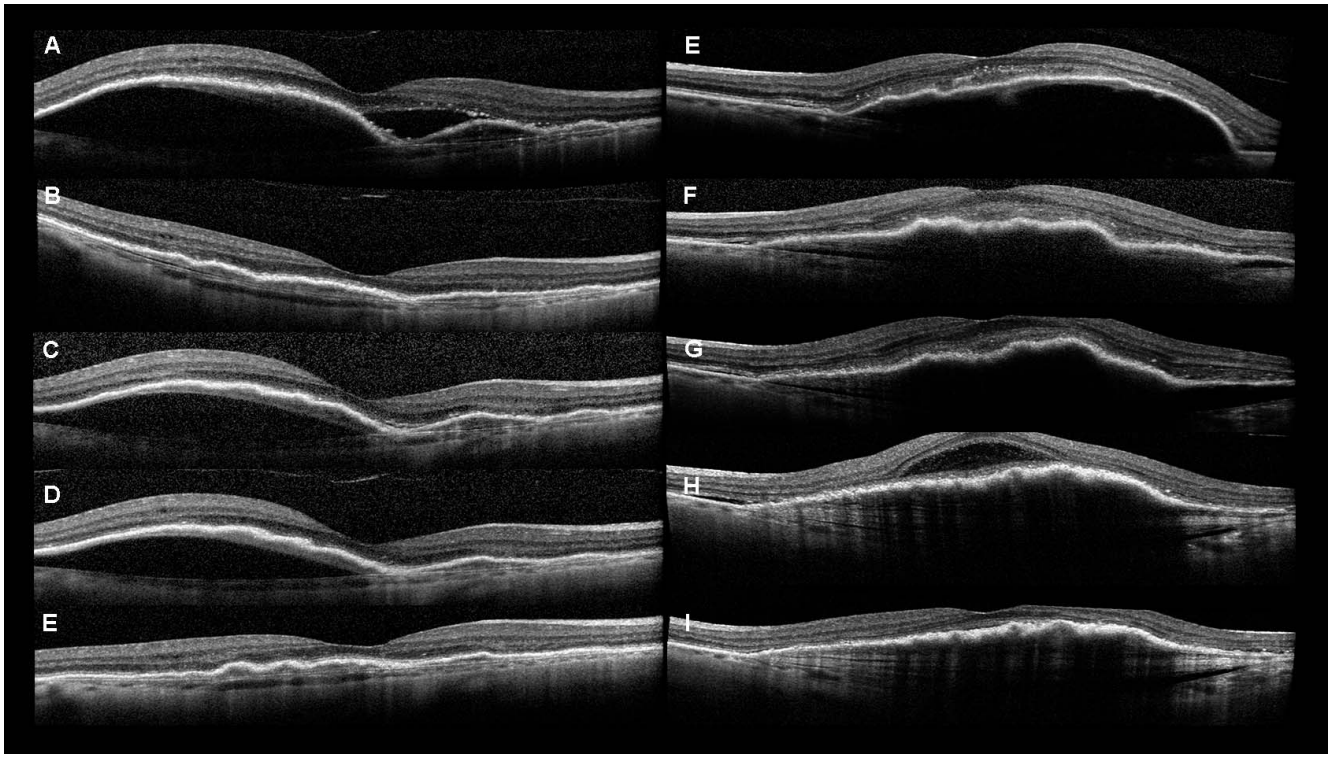

Figure 10. Registered cross-sectional OCT images from two patients with vsPED at baseline that evolved into fibrovascular PEDs with acute versus chronic height reduction. (**A**) OCT at baseline illustrates a type 1 neovascular membrane adjacent to a vsPED that reduces in height at 1 month (**B**) after the first injection. However, at the 2-month (**C**) and 4-month (**D**) follow-up visits, the serous component recurs despite two injections. At the 6-month follow-up, the PED once again reduces in height (**E**). With the second case, OCT at baseline illustrates a vsPED (**E**) that evolves into a multilayered morphology at the 3-month follow-up visit (**F**). Follow-up at 4 months (**G**), 1 year (**H**), and 2 years (**I**) illustrates stability of the multilayered fibrovascular PED with continuous injections.

the study period, may indicate that this PED group may be a more resistant subset. By contrast, the fibrovascular multilayered PEDs displayed more significant progression of the associated type 1 NV and a more stable anatomic outcome requiring fewer injections over time. Although visual outcomes were equivalent between the two groups, these findings may be limited by lead-time bias with transition of persistent vsPEDs into a multilayered fibrovascular PED beyond the follow-up period studied. Further studies to prospectively compare the two types of PEDs and their injection requirements and long-term final visual acuity may be warranted.

Acute versus chronic collapse of the PED may be the result of different mechanisms. In acute collapse, initial anti-VEGF therapy causes significant reduction in leakage and subsequent resorption of fluid. This acute mechanism may be more VEGF dependent in this immature phase. However, with continued injections, the effect of other profibrotic cytokines (e.g., platelet-derived endothelial cell growth factor or PDGF, connective tissue growth factor or CTGF) may supersede promoting maturation of the NV and evolution of the PED into a multilayered form.[13,31–33] Reduction in fibrovascular PED height in this context may be the result of fibrocytes and other inflammatory cells that contract, as evidenced by the presence of overlying RPE wrinkling.[34] Vascularized serous PEDs that acutely collapse because of VEGF-mediated reduction of fluid and leakage may transition to a chronic multilayered fibrovascular PED after chronic therapy.

It is unclear, however, why a significant proportion of vsPEDs persist (50% in our study). CNV/PED flow area ratio was greater in the multilayered fibrovascular PED group, which may be partly attributed to the greater fibrocellular component. It would seem that the persistent vsPED may harbor NV that is more resistant to fibrotic maturation, which could be due to the patient-specific cytokine or inflammatory milieu. As a result, the NV in persistent vsPEDs may remain more immature without sufficient structural support, leaving the endothelium prone to leakage.

RPE tear risk further supports the concept that all vsPEDs are a more unstable phenotype than their fibrovascular counterpart. While PED height over 550 μm is considered the greatest risk factor for RPE tear after anti-VEGF therapy, Chan et al. and others have noted that the NV to PED size ratio under 30% may represent an additional important risk factor.[29,35–41] Nagiel et al.[42] proposed an interplay of factors to explain the mechanism for RPE tear and suggested that RPE rips develop because of a combination of inward contraction of the NV due to unopposed anti-VEGF therapy and outward hydrostatic pressure in a PED at risk greater than 500 μm in height. In our series, both RPE tears developed in eyes with NV flow area less than 30%, emphasizing the concept that the vsPED may represent a more unstable form of PED in neovascular AMD. As these PEDs are at risk for an RPE tear, identification with OCTA may provide the retina specialist and patients additional information on the risks and benefits of anti-VEGF injection.

Limitations of this study were the retrospective design and relatively small sample size and the heterogenous cohort collected from multiple retinal centers. Not all patients were treatment naïve, and there were different treatment regimens employed with a varying number of prestudy treatments. It should be noted, however, that all patients were analyzed with the same OCTA algorithm and system and therefore the

analysis was remarkably consistent for all eyes included in this study. All OCTA algorithms, including the split-spectrum amplitude-decorrelation algorithm employed in this study, are unable to detect flow below a certain designated threshold, and therefore quantitative assessment of neovascular lesions may underestimate the true dimension of the NV complex. Additional limitations included the 1.5-year follow-up, which may have been insufficient to completely characterize the evolution of persistent vsPEDs to fibrovascular PEDs. Lead-time bias, however, is less likely to explain the findings given the significantly larger number of treatments prior to study enrollment in the persistent vsPED group. In any case, future studies with longer-term follow-up may be warranted. Definitive histopathologic analysis would be informative to confirm the morphologic NV changes that we have identified.

This study chronologically and serially analyzed OCTA images of vsPEDs associated with type 1 NV in the setting of intravitreal anti-VEGF therapy. We sequentially identified two dynamic morphologic outcomes of vsPED: multilayered filled fibrovascular PEDs versus persistent vsPEDs. The former typically reduced in height with resolution of the serous component and may represent a more stable anatomic outcome requiring a reduced injection burden versus the persistent vsPEDs, which may represent a more unstable morphology. Understanding these changes in the progression of the disease provides insight into the pathophysiology of vsPEDs and may refine our clinical approaches to this phenotype of neovascular AMD.

Acknowledgments

Supported by funding from Research to Prevent Blindness (DS) (New York, NY, USA) and the Macula Foundation, Inc. (DS) (New York, NY, USA).

Disclosure: **A. Au**, None; **K. Hou**, None; **J.P. Dávila**, None; **F. Gunnemann**: None, **S. Fragiotta**, None; **M. Arya**, None; **R. Sacconi**: None; **D. Pauleikhoff**, Novartis (R), Bayer (R), Heidelberg (R); **G. Querques**, None; **N. Waheed**, Optovue (S), Nidek (S), Heidelberg (C), Genentech (C), Janssen (C), Apellis (C), Ocudyne (S), Stealth (C), Zeiss (F), Topcon (F), Regeneron (C), Eleven (C), Boehringer-Ingelheim (C), Ocudyne (C), Galecto (C); **K.B. Freund**, Zeiss (C), Optovue (C), Genentech (C), Novartis (C), Genentech (F), Roche (F), Allergan (C), Heidelberg(C); **S. Sadda**, Allergan (C, F), Genentech (C, F), Iconic (C), Heidelberg (C), Optos (C), Carl Zeiss Meditec (F), Novartis (C), Centervue (C), Oxurion (C), Topcon (R); **D. Sarraf**, Amgen (C, F), Genentech (C, F), Heidelberg (F), Novartis (C, F), Optovue (C, F), Regeneron (F), Bayer (C, F)

References

1. Spaide RF. Enhanced depth imaging optical coherence tomography of retinal pigment epithelial detachment in age-related macular degeneration. *Am J Ophthalmol*. 2009;147:644–652.
2. Chevreaud O, Oubraham H, Cohen SY, et al. Ranibizumab for vascularized pigment epithelial detachment: 1-year anatomic and functional results. *Graefes Arch Clin Exp Ophthalmol*. 2017;255:743–751.
3. Solomon SD, Bressler SB, Hawkins BS, Marsh MJ, Bressler NM; Submacular Surgery Trials Research Group. Guidelines for interpreting retinal photographs and coding findings in the Submacular Surgery Trials (SST): SST report no. 8. *Retina*. 2005;25:253–268.
4. Punjabi OS, Huang J, Rodriguez L, Lyon AT, Jampol LM, Mirza RG. Imaging characteristics of neovascular pigment epithelial detachments and their response to anti-vascular endothelial growth factor therapy. *Br J Ophthalmol*. 2013;97:1024–1031.
5. Broadhead GK, Hong T, Zhu M, et al. Response of pigment epithelial detachments to intravitreal aflibercept among patients with treatment-resistant neovascular age-related macular degeneration. *Retina*. 2015;35:975–981.
6. Xu D, Davila JP, Rahimi M, et al. Long-term progression of type 1 neovascularization in age-related macular degeneration using optical coherence tomography angiography. *Am J Ophthalmol*. 2018;187:10–20.
7. Inoue M, Arakawa A, Yamane S, Kadonosono K. Variable response of vascularized pigment epithelial detachments to ranibizumab based on lesion subtypes, including polypoidal choroidal vasculopathy. *Retina*. 2013;33:990–997.
8. Ach T, Hoeh AE, Ruppenstein M, Kretz FTA, Dithmar S. Intravitreal bevacizumab in vascular pigment epithelium detachment as a result of subfoveal occult choroidal neovascularization in age-related macular degeneration. *Retina*. 2010;30:1420–1425.
9. Kang H, Byeon SH, Kim SS, Koh HJ, Lee SC, Kim M. Combining en face optical coherence tomography angiography with structural optical coherence tomography and blow flow analysis for detecting choroidal neovascular complexes in pigment epithelial detachments [published online ahead of print May 8, 2018]. *Retina*. doi:10.1097/IAE.0000000000002201.
10. Yüksel H, Türkcü FM, Şahin A, et al. One year results of anti-vegf treatment in pigment epithelial detachment secondary to macular degeneration. *Arq Bras Oftalmol*. 2013;76:209–211.
11. Broadhead GK, Hong T, Zhu M, et al. Response of pigment epithelial detachments to intravitreal aflibercept among patients with treatment-resistant neovascular age-related macular degeneration. *Retina*. 2015;35:975–981.
12. Subfoveal neovascular lesions in age-related macular degeneration: guidelines for evaluation and treatment in the Macular Photocoagulation Study. *Arch Ophthalmol*. 1991;109:1242–1257.
13. Rahimy E, Freund KB, Larsen M, et al. Multilayered pigment epithelial detachment in neovascular age-related macular degeneration. *Retina*. 2014;34:1289–1295.
14. Gass JDM. Serous retinal pigment epithelial detachment with a notch: a sign of occult choroidal neovascularization. *Retina*. 1984;4:205–220.
15. Jung JJ, Chen CY, Mrejen S, et al. The incidence of neovascular subtypes in newly diagnosed neovascular age-related macular degeneration. *Am J Ophthalmol*. 2014;158:769–779.
16. Guyer DR, Yannuzzi LA, Slakter JS, Sorenson JA, Hope-Ross M, Orlock DR. Digital indocyanine-green videoangiography of occult choroidal neovascularization. *Ophthalmology*. 1994;101:1727–1735.
17. Slakter JS, Yannuzzi LA, Schneider U, et al. Retinal choroidal anastomoses and occult choroidal neovascularization in age-related macular degeneration. *Ophthalmology*. 2000;107:724–753.
18. Baumal CR, Reichel E, Duker JS, Wong J, Puliafito CA. Indocyanine green hyperfluorescence associated with serous retinal pigment epithelial detachment in age-related macular degeneration. *Ophthalmology*. 1997;104:761–769.
19. Watzke RC, Klein ML, Hiner CJ, Chan BKS, Kraemer DF. A comparison of stereoscopic fluorescein angiography with indocyanine green videoangiography in age-related macular degeneration. *Ophthalmology*. 2000;107:1601–1606.
20. Cohen SY, Creuzot-Garcher C, Darmon J, et al. Types of choroidal neovascularisation in newly diagnosed exudative age-related macular degeneration. *Br J Ophthalmol*. 2007;91:1173–1176.
21. Yannuzzi LA, Hope-Ross M, Slakter JS, et al. Analysis of vascularized pigment epithelial detachments using indocyanine green videoangiography. *Retina*. 1994;14:99–113.

22. Mokwa NF, Ristau T, Keane PA, Kirchhof B, Sadda SR, Liakopoulos S. Grading of age-related macular degeneration: comparison between color fundus photography, fluorescein angiography, and spectral domain optical coherence tomography. *J Ophthalmol*. 2013;2013:385915.
23. Bressler NM; Treatment of Age-Related Macular Degeneration with Photodynamic Therapy (TAP) Study Group. Photodynamic therapy of subfoveal choroidal neovascularization in age-related macular degeneration with verteporfin: two-year results of 2 randomized clinical trials-tap report 2. *Arch Ophthalmol*. 2001;119:198–207.
24. Nagiel A, Sarraf D, Sadda SR, et al. Type 3 neovascularization: evolution, association with pigment epithelial detachment, and treatment response as revealed by spectral domain optical coherence tomography. *Retina*. 2015;35:638–647.
25. Spaide RF. Volume-rendered angiographic and structural optical coherence tomography. *Retina*. 2015;35:2181–2187.
26. Kuehlewein L, Bansal M, Lenis TL, et al. Optical coherence tomography angiography of type 1 neovascularization in age-related macular degeneration. *Am J Ophthalmol*. 2015;160:739–748.
27. Nagiel A, Sadda SR, Schwartz SD, Sarraf D. Resolution of giant pigment epithelial detachment with half-dose aflibercept. *Retin Cases Brief Rep*. 2015;9:269–272.
28. Grossniklaus HE, Gass JDM. Clinicopathologic correlations of surgically excised type 1 and type 2 submacular choroidal neovascular membranes. *Am J Ophthalmol*. 1998;126:59–69.
29. Sarraf D, Reddy S, Chiang A, Yu F, Jain A. A new grading system for retinal pigment epithelial tears. *Retina*. 2010;30:1039–1045.
30. Sadda SR, Guymer R, Holz FG, et al. Consensus definition for atrophy associated with age-related macular degeneration on OCT: Classification of Atrophy Report 3. *Ophthalmology*. 2018;125:537–548.
31. Schlingemann RO. Role of growth factors and the wound healing response in age-related macular degeneration. *Graefes Arch Clin Exp Ophthalmol*. 2004;242:91–101.
32. Green WR, Enger C. Age-related macular degeneration histopathologic studies: the 1992 Lorenz E. Zimmerman lecture. *Ophthalmology*. 1993;100:1519–1535.
33. Kuiper EJ, Van Nieuwenhoven FA, de Smet MD, et al. The angio-fibrotic switch of VEGF and CTGF in proliferative diabetic retinopathy. *PLoS One*. 2008;3:e2675.
34. Lam D, Semoun O, Blanco-Garavito R, et al. Wrinkled vascularized retinal pigment epithelium detachment prognosis after intravitreal anti-vascular endothelial growth factor therapy. *Retina*. 2018;38:1100–1109.
35. Sarraf D, Chan C, Rahimy E, Abraham P. Prospective evaluation of the incidence and risk factors for the development of RPE tears after high-and low-dose ranibizumab therapy. *Retina*. 2013;33:1551–1557.
36. Clemens CR, Wolf A, Alten F, Milojcic C, Heiduschka P, Eter N. Response of vascular pigment epithelium detachment due to age-related macular degeneration to monthly treatment with ranibizumab: the prospective, multicentre RECOVER study. *Acta Ophthalmol*. 2017;95:683–689.
37. Leitritz M, Gelisken F, Inhoffen W, Voelker M, Ziemssen F. Can the risk of retinal pigment epithelium tears after bevacizumab treatment be predicted? An optical coherence tomography study. *Eye*. 2008;22:1504–1507.
38. Doguizi S, Ozdek S. Pigment epithelial tears associated with anti-vegf therapy: incidence, long-term visual outcome, and relationship with pigment epithelial detachment in age-related macular degeneration. *Retina*. 2014;34:1156–1162.
39. Sarraf D, Joseph A, Rahimy E. Retinal pigment epithelial tears in the era of intravitreal pharmacotherapy: risk factors, pathogenesis, prognosis and treatment (an American ophthalmological society thesis). *Trans Am Ophthalmol Soc*. 2014;112:142–159.
40. Chiang A, Chang LK, Sarraf D. Predictors of anti-VEGF-associated retinal pigment epithelial tear using FA and OCT analysis. *Retina*. 2008;28:1265–1269.
41. Chan CK, Meyer CH, Gross JG, et al. Retinal pigment epithelial tears after intravitreal bevacizumab injection for neovascular age-related macular degeneration. *Retina*. 2007;27:541–551.
42. Nagiel A, Freund KB, Spaide RF, Munch IC, Larsen M, Sarraf D. Mechanism of retinal pigment epithelium tear formation following intravitreal anti-vascular endothelial growth factor therapy revealed by spectral-domain optical coherence tomography. *Am J Ophthalmol*. 2013;156:981–988.

Investigative Ophthalmology & Visual Science